Multi-scale characterization by neutronography and electron diffraction of Ni coating on Cu-Ni-Al or cast-iron glass molds after laser cladding

Fazati Bourahima, Anne-Laure Helbert, Frédéric Ott, Vincent Ji, Michel Rege, François Brisset, Arnaud Courteaux, Thierry Baudin

Multi-scale characterization by neutronography and electron diffraction of Ni coating on Cu-Ni-Al or cast-iron glass molds after laser cladding

Fazati Bourahima[1, 2, a *], Anne-Laure Helbert[2, b], Frédéric Ott[3, c], Vincent Ji[2, d], Michel Rege[1, e], François Brisset[2, f], Arnaud Courteaux[1, 2, g], Thierry Baudin[2, h]

[1] Etablissements Chpolansky, 91462 Marcoussis, France

[2] Université Paris-Saclay, CNRS, Institut de chimie moléculaire et des matériaux d'Orsay, 91405, Orsay, France

[3] LLB - Laboratoire Léon Brillouin, UMR12 CEA-CNRS, Bât. 563 CEA Saclay, 91191 Gif sur Yvette Cedex, France

[a*]fazati.bourahima@chpolansky.fr, [b]anne-laure.helbert@u-psud.fr, [c]frederic.Ott@cea.fr, [d]vincent.ji@u-psud.fr, [e]michel.rege@chpolansky.fr, [f]francois.brisset@u-psud.fr, [g]arnaud.courteaux@orange.fr, [h]thierry.baudin@u-psud.fr

Keywords: Laser cladding, Multi-scale analysis, Neutronography, MEB/EDS/EBSD

Abstract.
Laser cladding of a Ni based powder on Cu-Ni-Al or cast iron was performed with a 4kW continuous Nd: YAG laser. The Cu-Ni-Al and cast-iron substrates are used for their thermal properties in glass mold industry. But the issue of these materials is their lack of resistance on corrosion and abrasion. The role of the Ni based alloy is to protect the mold without affecting its thermal properties (Heat Affected Zone (HAZ)). The purpose of this research is to produce a well bonded Ni based melted powder without pores or cracks on a non-planar surface (curvilinear section). An investigation of the impact of the processing parameters, power (1500-3200 W), scanning speed (2.5-10 mm/s) and powder feeding rate (24.5-32.5 g/min) on the bonding quality, the porosity propagation and HAZ appearance is performed. The used methods are neutronography, Scanning Electron Microscopy, Energy Dispersive Spectroscopy and Electron BackScatter Diffraction (EBSD). These multi-scale techniques are obviously complementary. Neutronography is a well-adapted non-destructive method to observe the porosity in the volume thanks to the contrast between materials. EBSD analysis allows us to analyze the microstructural evolution of the coating notably by observing the dendrites growth. This same method also permits to observe the HAZ nature according to the laser cladding parameters. Those methods allowed to optimize the processing parameters in a way to obtain perfect bonding, to avoid porosity propagation and to limit the HAZ emergence.

Introduction

The Laser Metal Deposition (LMD) technique allows to direct the powder but also the laser to one focal point. The melting–solidification of the powder, projected by a nozzle usually coaxial happens in the same time as it is deposited in the substrate. The laser produces a melt pool to create a layer and raise the global volume. In this case the application is surface treatment (cladding) and/or parts repair. This method is well known for additive manufacturing [1]. In glass industry, the glass production induces a high mechanical and thermal damage on molds. Therefore, they need to be protected. The most famous techniques used to do so are: Plasma Transferred Arc (PTA) and blowtorch [2]. But with those techniques, a high Heat Affected Zone (HAZ) is created. The LMD is today an interesting alternative for this surface treatment. In many papers this technique have proven its efficiency because of its low HAZ and

the bonding quality improvement [3]. Also, the mechanical behavior of this method has been observed to be more efficient than the PTA or Tungsten Inert Gaz (TIG) techniques [4]. A lot of works have presented the impact of laser process on the microstructural but also thermomechanical behavior of the coating and the substrate [5][6][7]. For example, they have noticed a limited formation of martensite in the cast iron substrate after cladding. To do so, many characterization methods have been used: Scanning Electron Microscopy (SEM), microhardness, calorimeter, etc. In the present paper, a combination of different characterization techniques is presented. So, it can be possible to represent the influence of the processing parameters on the macrostructural and microstructural features. Especially, neutronography, a technique based on neutron diffraction [8] coupled with the tomography principle [9], is used to allow us to optimize the laser cladding conditions.

Material and experimental techniques

A 4KW Nd: YAG laser with a wavelength of 1033 nm is used. An optical fiber with a diameter of 600 µm is used for guiding the beam. A 3-jet nozzle allows to direct the powder to the focal point for the fusion and solidification. The Ni based powder, the Cu-Ni-Al and Grey Cast-Iron chemical compositions are listed in Table 1. The substrate materials are chosen for their good thermal properties [2]. Indeed, they are important to insure a homogeneous heat transfer between the mold and the glass bottle during the production. Then, they must absorb homogenously the heat produced by the viscous glass to obtain a bottle without inhomogeneous thickness and cracks.

Table 1: Chemical composition of the substrates and powder (wt%)

Chemical elements	Fe	Mn	Al	Ni	Zn	Pb	Sn	Si	Cu	B	Cr	C	S	P
Cu-Ni-Al	<1	0.5	8.5	15	8	<0.1	0.15	1	Bal.	-	-	-		
Grey Cast Iron	Bal.	0.2-1										2.5- 4	0.02-0.25	0.02-1
Ni powder	1	0.1	-	Bal.	-	-	-	2.5	-	1.7	0.3	0.5	-	-

Several sets of laser cladding processing parameters were studied in a recent study [10]. Two of them are used in the present paper for each substrate to discuss the impact of the processing parameters and especially the laser power on the default appearance (Table 2).

Table 2: Processing parameters of the studied samples for Cu-Ni-Al and Cast Iron

Sample	**Power P (W)**	**Scanning speed v (mm/s)**	**Powder feeding rate PFR (g/min)**	**Spot diameter D (mm)**
Cu-Ni-Al 1	3200	10	28.5	4
Cast Iron 1	1900	6.5		
Cast Iron 2	3100			

A half of a Cast Iron mold is presented in Fig. 1 with the description of the analyzed zones: the coating in 3D (Fig. 1a) for neutronography and a cross section (Fig.1b) for SEM observations. The same protocol is applied to the Cu-Ni-Al glass mold.

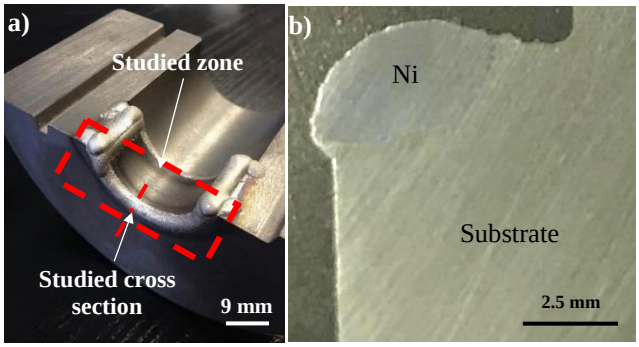

Figure 1: Half of a necking mold with a) the coating to be observed in 3D and b) the cross section

In order to observe the effect of the processing parameters on the coating behavior and on the microstructural evolution, different analyses have been done. For macrostructural analysis, neutronography is performed. It is a nondestructive analysis. The selected part (discontinuous red rectangle in Fig 1.a) is mechanically cut, then the obtained sample is placed between a detector and the neutron source [8]. The distance from the detector to the neutron source is 4 m. The analysis is called *Prompt-Gamma Activation Analysis* (PGAA) [8]. The sample absorbs the neutrons and then emits prompt gamma rays. Those gamma rays are measured by the detector. The result is obtained by image reconstruction [8].

For microstructural analysis, the sample (cross section in Fig. 1b) is polished with SiC papers and then using diamond suspensions until 1 µm for optical microscopy analysis and finally with OPS suspension for SEM observations and EBSD and EDS (Energy Dispersive Spectroscopy) analyses.

Results and discussion

Macroscopical neutronography observations

For Cast Iron 1 sample, the 3D coating (Fig. 1a) can be observed thanks to the VolView 3.4 software [11] in Fig. 2a. From this 3D image, the ImageJ software allows to do the sample reconstruction slice by slice in order to observe inside the coating. Fig. 2b to 2g allow to see the mold (in black) and the coating (in white) at several locations. It is possible to see voids inside the coating section by section.

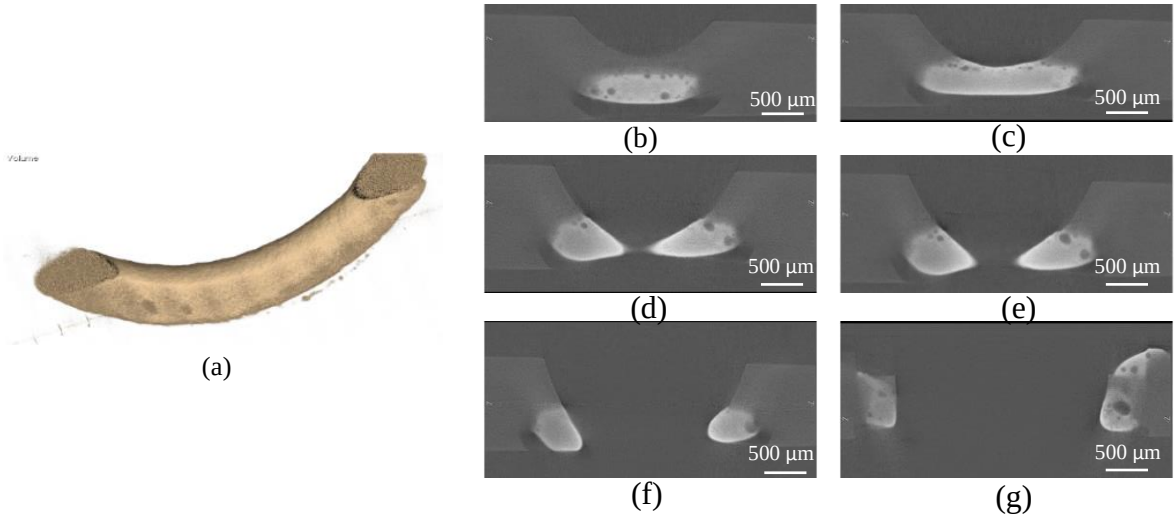

Figure 2: (a) 3D image of the coating (see Figure 1a) obtained with VolView 3.4. Observations of the Cast Iron 2 sample after neutronography and ImageJ treatment: different slices of imageJ reconstruction (b)-(c) curved center, (d)-(e) away from the curved center and (f)-(g) close to the edges.

The porosity size is about 30 µm but can reach about 200 µm for the highest laser power (Cast Iron 2) [10]. This result means that increasing the power induces porosity formation due to the high generated temperature. Let us note that at this measure scale, the bonding seems perfect.

In conclusion, a compromise needs to be found between a perfect bonding and a coating without porosity, indeed, for low power conditions, the porosity size remains very low in all cases (under 40 µm) but the bonding can be defective for the Ni coating on the Cu-Ni-Al substrate even if the porosity size remains very low in all cases (under 40 µm). Finally, power must be minimized but still sufficient to guaranty the bonding that can be finely analyzed from a microstructural point of view.

Microstructural analysis

Microstructural analysis was done by SEM on a section at the curvature after cladding of Ni based powder on a Cu-Ni-Al mold (Fig. 3) and allows to observe the bonding quality as well as the Ni solidification structure.

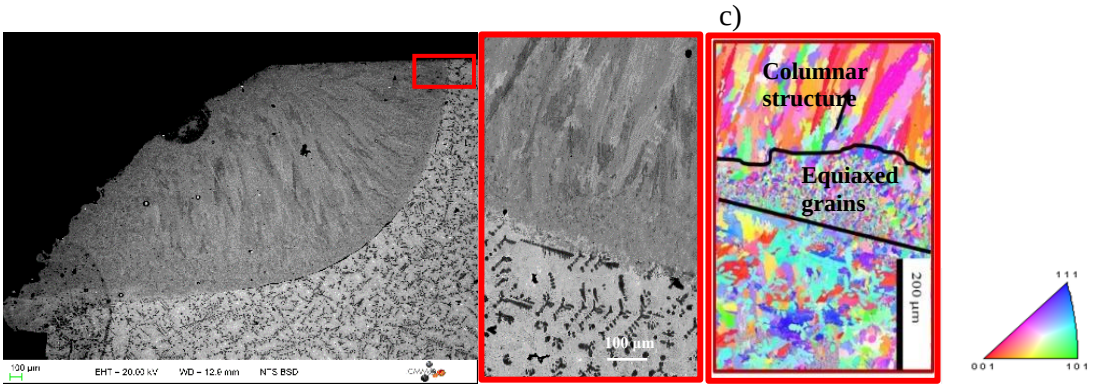

Figure 3: Micrography of the sample Cu-Ni-Al 1 after cladding (a)-(b) SEM of the section after Ni coating on Cu-Ni-Al substrate (b corresponds to the red square in Fig 3a which is rotated) and (c) EBSD analysis: Inverse Pole Figure of the same area

The SEM-BSD-EBSD analysis presented in Fig. 3 shows in detail the solidification structure but also the impact of laser cladding on the microstructural behavior. In the coating (Fig. 3a) three structures can be described: equiaxed grains close to the interface (average size of 6 µm) which correspond to a heterogeneous nucleation, then columnar dendrites in the <001> directional growth is observed (Fig. 3c) and finally, equiaxed grains at the extreme surface. A lack of bonding due to the high laser speed (Table 2) is observed in the section curved center (Fig. 3a). But a perfect bonding is present on the edges. To analyze the bonding, the dilution zone (DZ) thickness has been carried out thanks to chemical analysis (EDS) (Fig. 4). Fig.4b shows a decrease of the Ni element from the coating to the substrate. At the same time, the Cu composition progressively increases.

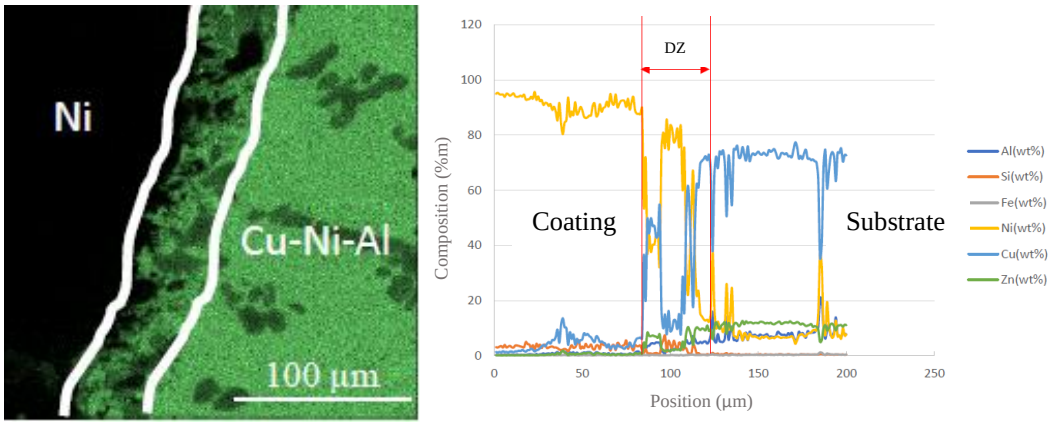

Figure 4: MEB-EDS observation after cladding of Cu-Ni-Al 1 (a) EDS cartography of Cu element at the edge and (b) chemical line observation from the coating to the substrate

So, from the analysis of the Fig. 4, it is possible to see that the bonding is present when the chemical dilution is observed (here with a thickness of about 35 µm). An optimization of the process parameters to observe a perfect bonding all along the section and to respect the coating geometry without porosities gave the following values [10]: P=2900W, v=7.5 mm/s and PFR=27.5 g/min.

A SEM-BSD-EBSD analysis after cladding of Ni based powder on a Cast Iron mold is also presented in Fig. 5.

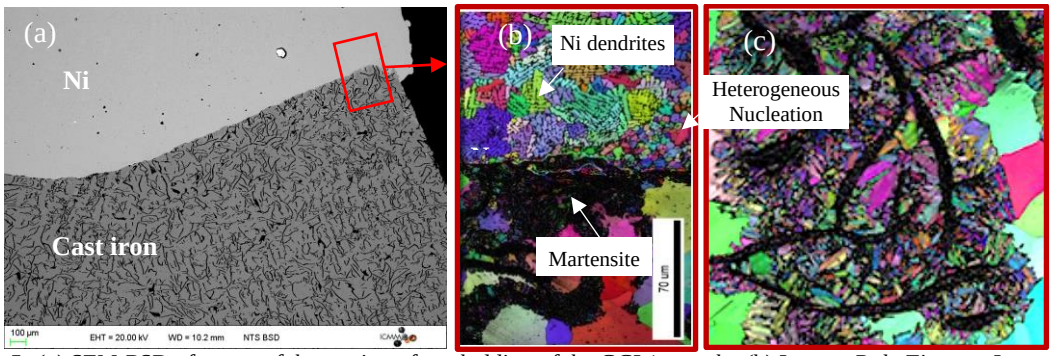

Figure 5: (a) SEM-BSD of a part of the section after cladding of the GCI 1 sample, (b) Inverse Pole Figure +Image Quality of the edge (red square in Fig. 5a) and c) magnification of martensite shown in Fig. 5b

Fig. 5a allows to observe a high bonding quality and a coating with low porosity. Also, the SEM observation shows the lamellar graphite inside the ferritic matrix. From the Fig. 5b, several information can be noticed: close to the interface, in the coating, heterogeneous nucleation is present (right side of Fig. 5b) when in the substrate, ferritic grains can be observed but also lamellar graphite surrounded by needle. Those needles are characteristic of martensite formation and represent the HAZ. This martensite is characteristic of carbon diffusion at high temperature provided by the laser followed by a very high cooling rate ($\approx 1.8.10^3$ K/s) as described by Liu et al. [5]. The martensite, according to its hardness can lead to cracking. An optimization of the process to observe a coating without porosities and low HAZ (lower than 100 µm size) gave the following parameters [10]: P=1900W, v=7.5 mm/s and PFR=28.5 g/min. Let us remark finally that a lower power is needed to obtain a perfect bonding on Cast Iron because of the high absorptivity of the iron ($\approx$ 0.3) compared to the low absorptivity of the Cu mold ($\approx$ 0.06).

Conclusion

In this paper, a multiscale analysis of Ni coating on Cu-Ni-Al or Cast-iron glass molds after laser cladding was performed. The research results are as follows:

1. Neutronography is a non-destructive efficient analysis to observe the defaults in the volume such as porosity in the coating.
2. It was shown that a good bonding is possible between substrate and coating thanks to the chemical dilution over about 35 µm which can be achieved when laser power is sufficient (1900 W for Cast-iron and 2900 W for Cu-Ni-Al).
3. EBSD allowed to verify the solidification direction (<001>) of the Ni dendrite of the coating but also the martensite formation mixed with the ferrite grains inside the Cast Iron substrate close to the interface.
4. From these multi-scale analysis, optimized laser cladding parameters have been determined to insure a perfect bonding and a coating without porosities.

References

[1] T. DebRoy, H.L. Wei, J.S. Zuback, T. Mukherjee, J.W. Elmer, J.O. Milewski, A.M. Beese, A. Wilson-Heid, A. De, W. Zhang, Additive manufacturing of metallic components – Process, structure and properties, Prog. Mater. Sci. 92 (2018) 112–224. doi:10.1016/j.pmatsci.2017.10.001.

[2] M. Rege, S. Van Linden, Stage de formation aux techniques de rechargement dans l'industrie verrière, Marcoussis, 2016.

[3] F. Bourahima, A.L. Helbert, M. Rege, V. Ji, D. Solas, T. Baudin, Laser cladding of Ni based powder on a Cu-Ni-Al glassmold: Influence of the process parameters on bonding quality and coating geometry, J. Alloys Compd. 771 (2019) 1018–1028. doi:10.1016/j.jallcom.2018.09.004.

[4] G. Xu, M. Kutsuna, Z. Liu, K. Yamada, Comparison between diode laser and TIG cladding of Co-based alloys on the SUS403 stainless steel, Surf. Coatings Technol. 201 (2006) 1138–1144. doi:10.1016/j.surfcoat.2006.01.040.

[5] H. Liu, J. Hao, Z. Han, G. Yu, X. He, H. Yang, Microstructural evolution and bonding characteristic in multi-layer laser cladding of NiCoCr alloy on compacted graphite cast iron, J. Mater. Process. Technol. 232 (2016) 153–164. doi:10.1016/j.jmatprotec.2016.02.001.

[6] F. Fu, Y. Zhang, G. Chang, J. Dai, Analysis on the physical mechanism of laser cladding crack and its influence factors, Optik (Stuttg). 127 (2016) 200–202. doi:10.1016/j.ijleo.2015.10.043.

[7] P. Yi, X. Zhan, Q. He, Y. Liu, P. Xu, P. Xiao, D. Jia, Influence of laser parameters on graphite morphology in the bonding zone and process optimization in gray cast iron laser cladding, Opt. Laser Technol. 109 (2019) 480–487. doi:10.1016/j.optlastec.2018.08.028.

[8] G. Pépy, Spectrométrie masse - principe neutrons - analyse et appareillage par : les faisceaux de neutrons analyse des traces , imagerie et médecine, Tech. l'ingénieur. V1 (2006) 1–8.

[9] C. Thiery, Tomographie à rayons X, Tech. l'ingénieur. P950 V3 (2013) 1–30.

[10] F. Bourahima, Évolutions microstructurales et défauts générés par laser cladding lors du dépôt de Ni sur des moules de verrerie en alliage de Cu-Ni-Al et en fonte GL, Thèse Université Paris-Sud, To cite this version : HAL Id : tel-02044203, 2019.

[11] DRSN/SEROS, http://www-llb.cea.fr/neutrono/radio-neut.html, (2016). http://www-llb.cea.fr/neutrono/radio-neut.html.